# The Generality of Architectural Isomerism in Designer Inclusion Frameworks

**K. Travis Holman,† Stephen M. Martin, Daniel P. Parker,§ and Michael D. Ward***

*Contribution from the Department of Chemical Engineering and Materials Science, University of Minnesota, Amundson Hall, 421 Washington Avenue, SE, Minneapolis, Minnesota, 55455*

*Received August 14, 2000. Revised Manuscript Received December 6, 2000*

**Abstract:** We describe herein new structural isomers of a lamellar host system based on organodisulfonate "pillars" that connect opposing hydrogen-bonded sheets, consisting of topologically complementary guanidinium (**G**) ions and sulfonate (**S**) groups, to generate inclusion cavities between the sheets. These new isomers—zigzag brick, double brick, V-brick, and crisscross bilayer—expand significantly on our earlier report of architectural isomerism displayed by the discrete bilayer and simple brick forms. We demonstrate here that the discrete bilayer−simple brick isomerism, which was limited to several host−guest combinations based on the $\mathbf{G}_2$(4,4′-biphenyldisulfonate) host and one pair of compounds based on the $\mathbf{G}_2$(2,6-naphthalenedisulfonate), can be generalized to other organodisulfonate pillars. Furthermore, in many cases the selectivity toward the different framework isomers reflects a rather systematic templating role of the guest molecules and host−guest recognition during assembly of the lattice. We also describe a convenient approach to identifying and classifying the innumerable possible host architectures based upon the pillar projection topologies for the **GS** sheets and the intersheet connectivities. The discovery of these new architectures reveals a structural versatility for this class of materials that exceeds initial expectations and observations. Each topology produces different connectivities between the sheets in the third dimension that endows each framework isomer with uniquely shaped and sized inclusion cavities, enabling this host system to conform readily to different guests. The unlimited number of architectures available, combined with the inherent conformational softness and structural tunability of these host lattices, suggests a near universality for the **GS** system with respect to guest inclusion.

## Introduction

Crystalline inclusion compounds[1] are of considerable interest because of their potential use in applications such as optoelectronics, chemical separations, storage of sensitive compounds, and nanoconfined chemical reactions. Consequently, numerous strategies for designer organic host lattices are being explored.[2] The realization of inclusion compounds, however, can be difficult, owing to the relatively narrow distribution of guest sizes and shapes that typically can be included within a given host framework. Like crystalline organic solids in general, structural modifications of the molecular components of a host usually lead to unpredictable and often undesirable changes in crystal architecture, frustrating systematic control of structural features such as inclusion cavity size and shape, and frequently resulting in loss of inclusion behavior. In principle, these obstacles can be surmounted with a host system based on *structurally* persistent supramolecular building blocks *equipped with components that can be interchanged with retention of the general structural features and supramolecular connectivity of the host lattice*.

Over the past few years, we have reported inclusion compounds based on lamellar host frameworks constructed from guanidinium and organodisulfonate ions that embody the central axiom of crystal engineering[3]—the systematic design and predictable synthesis of solid state structures through judiciously chosen molecular components.[4] The organic residues of the organodisulfonate ions in these host frameworks serve as molecular "pillars" that connect opposing hydrogen-bonded sheets (Scheme 1) of complementary guanidinium (**G**) ions and sulfonate (**S**) moieties, thereby producing inclusion cavities

* To whom correspondence should be addressed. E-mail: wardx004@tc.umn.edu.

† Natural Sciences and Engineering Research Council (NSERC) of Canada Postdoctoral Fellow.

§ University of Minnesota Materials Research Science and Engineering REU Fellow.

(1) For an introduction to organic inclusion compounds, see: (a) Weber, E. In *Topics in Current Chemistry*; Springer-Verlag: Berlin, 1987; Vol. 140. (b) *Comprehensive Supramolecular Chemistry*; Atwood, J. A., Davies, J. E. D., NacNicol, D. D., Vögtle, F., Lehn, J.-M., Eds.; Elsevier Science: New York, 1996; Vol. 6. (c) *Inclusion Compounds. Structural Aspects of Inclusion Compounds Formed by Organic Host Lattices*; Atwood, J. A., Davies, J. E. D., MacNicol, D. D., Eds.; Academic: London, 1984; Vol. 2. (d) Bishop, R. *Chem. Soc. Rev.* **1996**, 311−319.

(2) (a) Aoyama, Y. In *Topics in Current Chemistry*; Springer-Verlag: Berlin, 1998; Vol. 198, p 131. (b) Endo, K.; Ezuhara, T.; Koyanagi, M.; Masuda, H.; Aoyama, Y. *J. Am. Chem. Soc.* **1997**, *119*, 499. (c) Aoyama, Y.; Endo, K.; Anzai, T.; Yamaguchi, Y.; Sawaki, T.; Kobayashi, K.; Kanehisa, N.; Hashimoto, H.; Kai, Y.; Masuda, H. *J. Am. Chem. Soc.* **1996**, *118*, 5562. (d) Toda, F. In *Inclusion Compounds*, Atwood, J. A., Davies, J. E. D., MacNicol, D. D., Eds.; Oxford University Press: 1991; Vol. 4. (e) Caira, M. R.; Nassimbeni, L. R.; Toda, F.; Vujovic, D. *J. Am. Chem. Soc.* **2000**, *122*, 9367. (f) Ermer, O. *Helv. Chim. Acta* **1991**, *74*, 825. (g) Ermer, O. *J. Am. Chem. Soc.* **1988**, *110*, 3747. (h) Wang, X.; Simard, M.; Wuest, J. D. *J. Am. Chem. Soc.* **1994**, *116*, 12119. (i) Brunet, P.; Simard, M.; Wuest, J. D. *J. Am. Chem. Soc.* **1997**, *119*, 2737. (j) Biradha, K.; Dennis, D.; MacKinnon, V. A.; Sharma, C. V. K.; Zaworotko, M. J. *J. Am. Chem. Soc.* **1998**, *120*, 11895.

(3) (a) Schmidt, G. M. J. *Pure. Appl. Chem.* **1971**, *27*, 647. (b) Desiraju, G. R. *Crystal Engineering: The Design of Organic Solids*; Elsevier: New York, 1989.

(4) (a) Russell, V. A.; Evans, C. C.; Li, W.; Ward, M. D. *Science* **1997**, *276*, 575. (b) Swift, J. A.; Reynolds, A. M.; Ward, M. D. *Chem. Mater.* **1998**, *10*, 4159. (c) Swift, J. A.; Ward, M. D. *Chem. Mater.* **2000**, *12*, 1501. (d) Evans, C. C.; Sukarto, L.; Ward, M. D. *J. Am. Chem. Soc.* **1999**, *121*, 320.

10.1021/ja0030257 CCC: $20.00 
Published on Web 04/19/2001

**Scheme 1**

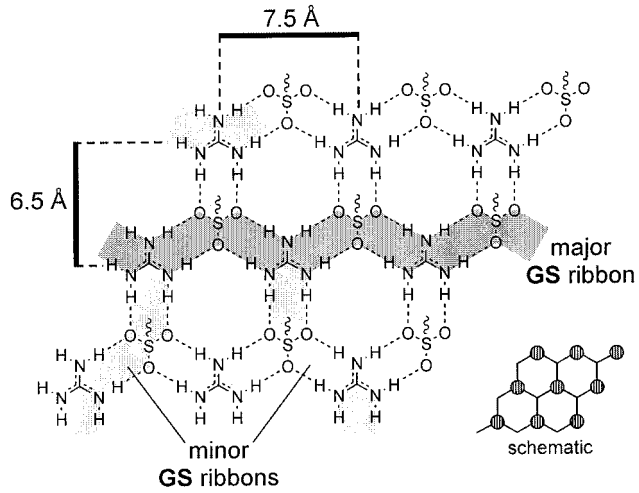


**Scheme 2**

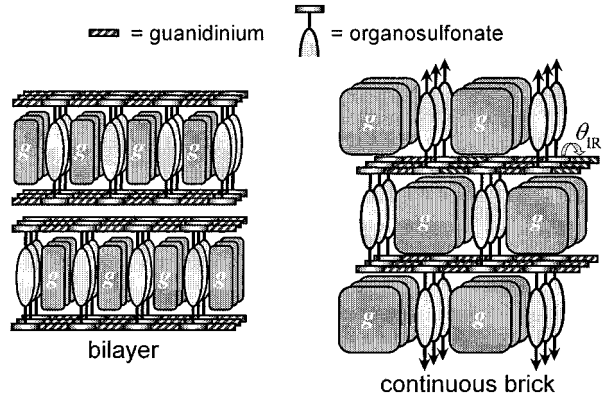


between the **GS** sheets. The **GS** sheets are highly persistent, and more important, the size and character of the inclusion cavities can be manipulated by the choice of organodisulfonate pillar without disrupting the supramolecular connectivity of the **GS** sheet.

We also reported that inclusion compounds based on one particular **GS** host, namely **$G_2$BPDS** (**BPDS** = 4,4′-biphenyldisulfonate), exhibit either a discrete "bilayer" or a continuous "brick" (hereafter referred to as "simple brick") architecture (Scheme 2), wherein the selectivity for these framework isomers appeared to be governed by the templating action of the guest molecules.[5,6] We characterized this phenomenon as "architectural isomerism," a term that we reserve for structural isomers that have the *same* compositions *and* identical, well-defined supramolecular connectivities (e.g., the H-bonded **GS** sheet), but differ with respect to the geometrical arrangements, or topologies, of the chemical subunits.[7] Pursuant to our initial observation of architectural isomerism, we reported one example of each of these two architectures for the **$G_2$NDS** host (**NDS** = 2,6-naphthalenedisulfonate).[8]

The different connectivities in the third dimension exhibited by the bilayer and simple brick isomers are achievable because the organodisulfonate pillars can extend from either side of the **GS** sheet. In the bilayer form the pillars project from the same side of each sheet, forming bilamellae that are discrete in the third dimension. The simple brick architecture, however, is continuous in 3-D because pillars projecting from both sides of each **GS** sheet connect adjacent sheets. The fundamental difference between the bilayer and simple brick architectures is, therefore, associated with the different up/down projections of the pillars from the **GS** sheets, or equivalently, their "projection topologies."

Architectural isomerism has been observed in several other hydrogen-bonded compounds[9] and appears to have important ramifications for inclusion behavior. The number of isomers within each system, however, generally is limited. For example, 1,3-cyclohexanedione can exist in two crystalline architectures, a guest-free 1-D hydrogen-bonded chain or a discrete host−guest cycla[6]mer,[9a] wherein identical tautomeric forms of the molecule are connected by the same O−H···O═C hydrogen bonds. Metal−organic frameworks can also exhibit architectural isomerism,[10] as exemplified by $[Co(4,4'\text{-bipyridine})_{1.5}(NO_3)_2]_n$, which exhibits three architectural isomers—ladder, bilayer, and modified brick wall—with different geometrical arrangements of the same T-shaped module.[10a−c]

We describe herein (i) the discovery of several new **GS** architectures—zigzag brick, double brick, and V-brick—that add to the aforementioned discrete bilayer and simple brick forms and suggest that the number of architectures available to this system is substantial, (ii) a convenient approach to identifying and classifying these host architectures based upon their pillar projection topologies and intersheet connectivities, (iii) architectural *isomerism* in **$G_2$BPDS**, **$G_2$NDS**, and several new **GS** hosts based on other organodisulfonate pillars, expanding significantly our previous observations and demonstrating the generality of this phenomenon, and (iv) unambiguous evidence for guest-templating and host−guest recognition during host framework assembly. The discovery of these new architectures reveals a structural versatility for this class of materials that exceeds initial expectations and observations. Each topology produces different connectivities between the sheets in the third dimension that endows each framework isomer with uniquely shaped and sized inclusion cavities, enabling this host system to conform readily to different guests. The innumerable number of possible architectures, combined with the inherent confor-

(5) Swift, J. A.; Pivovar, A. M.; Reynolds, A. M.; Ward, M. D. *J. Am. Chem. Soc.* **1998**, *120*, 5887.

(6) Holman, K. T.; Pivovar, A. M.; Swift, J. A.; Ward, M. D. *Acc. Chem. Res*. **2001**, *34*, 107.

(7) Architectural isomerism can be considered a subset of "supramolecular isomerism". Supramolecular isomerism (see Henniger, T. L.; MacQuarrie, D. C.; Losier, P.; Rogers, R. D.; Zaworotko, M. J. *Angew. Chem., Int. Ed. Engl*. **1997**, *36*, 972) encompasses structural isomers in which the supramolecular bonding motifs may be the same *or* different. By this definition, supramolecular isomerism is ubiquitous, as it includes polymorphs and solvates in addition to architectural isomers. Architectural isomerism can be further distinguished by comparison with host lattices that do not strictly fulfill the criterion. Although the substituted resorcinol host in reference 2b may appear to exhibit architectectural isomerism, the two types of inclusion compounds differ only with respect to a shift registry of the 1-D hydrogen-bonded chains and are not architectural isomers. Different host architectures in ref 2c are achieved by changing the host components, but these hosts are not isomers because their chemical compositions differ.

(8) Holman, K. T.; Ward, M. D. *Angew. Chem., Int. Ed*. **2000**, *39*, 1653.

(9) (a) Etter, M. C.; Urbanczyk-Lipkowska, Z.; Jahn, D. A. *J. Am. Chem. Soc*. **1986**, *108*, 5871. (b) MacGillivray, L. R.; Diamente, P. R.; Reid, J. L.; Ripmeester, J. A. *Chem. Commun*. **2000**, 359. (c) MacGillivray, L. R.; Atwood, J. L. *J. Am. Chem. Soc*. **1997**, *119*, 6931. (d) MacGillivray, L. R.; Holman, K. T.; Atwood, J. L. *Cryst. Eng.* **1998**, *1*, 87−96. (e) Herbstein, F. H. In *Topics in Current Chemistry*; Springer-Verlag: Berlin, 1987; Vol. 140.

(10) (a) Losier, P.; Zarowotko, M. J. *Angew. Chem., Int. Ed. Engl*. **1996**, *35*, 2779. (b) Power, N. K.; Hennigar, T. L.; Zaworotko, M. J. *New J. Chem*. **1998**, *22*, 177. (c) Gudbjartson, H.; Biradha, K.; Poirier, K. M.; Zaworotko, M. J. *J. Am. Chem. Soc*. **1999**, *121*, 2599. (d) Kasai, K.; Aoyagi, M.; Fujita, M. *J. Am. Chem. Soc.* **2000**, *122*, 2140. (e) Battan, S. R.; Robson, R. *Angew. Chem., Int. Ed.* **1998**, *37*, 1460. (f) Hagerman, P. J.; Hagerman, D.; Zubieta, J. *Angew. Chem., Int. Ed.* **1999**, *38*, 2638. (g) Li, H.; Yaghi, O. M. *J. Am. Chem. Soc*. **1998**, *120*, 10569. (h) O'Keefe, M.; Yaghi, O. M. *Eur. Chem. J.* **1999**, *5*, 2796.

**Scheme 3**

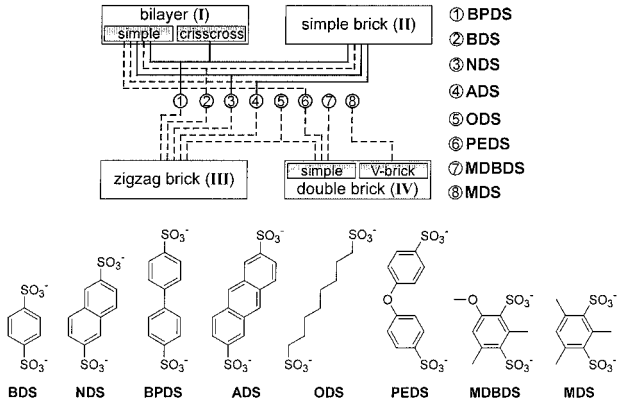


mational softness and structural tunability of these host lattices, suggests a near universality for the **GS** system with respect to guest inclusion.

## Results and Discussion

**Generality of Bilayer−Brick Isomerism and New Brick Architectures.** Previous work in our laboratory with **GS** inclusion compounds based on **BPDS** established architectural isomerism between the bilayer and "simple" brick frameworks.[5,6] These investigations, and complementary studies based on 4,4′-azobenzenedisulfonate (**ABDS**) and 2,6-naphthalenedisulfonate (**NDS**) pillars,[4d,8] have suggested that bilayer−brick isomerism may be governed by the combined steric demands of the pillars and guests in the gallery regions between the **GS** sheets. The generality of this phenomena is demonstrated herein by several new examples of bilayer and simple brick host frameworks constructed with **BPDS**, **NDS**, 1,4-benzenedisulfonate (**BDS**), and 2,6-anthracenedisulfonate (**ADS**) pillars, as well as the by the observation of new architectural isomers with these and other pillars. Scheme 3 illustrates, in overview form, the extent to which the results reported herein expand upon our previously reported efforts. The dashed lines in Scheme 3 represent architectures that have been reported previously, whereas the solid lines represent the new examples. This scheme illustrates that architectural isomerism, wherein more than one isomer is observed for a given host composition, has been limited to the **G$_2$BPDS** and **G$_2$NDS** hosts. With the exception of **G$_2$MDBDS** and **G$_2$MDS**, the scheme illustrates that some form of architectural isomerism has now been demonstrated for each host described here. This illustrates the generality of architectural isomerism and the likelihood that all of the architectures in Scheme 3, as well as ones yet undiscovered, are achievable for numerous organodisulfonate pillars.

**Systematic Architectural Isomerism with Arene Pillars.** With small guests such as tetrahydrofuran (volume of guest, $V_g = 73$ Å$^3$)[11] the smallest pillar, **BDS**, adopts a typical bilayer framework with quasihexagonal **GS** sheets.[12] The guests in **G$_2$BDS**·(*tetrahydrofuran*) are included in cavities flanked by the **BDS** pillars, whose molecular planes are orthogonal to the major **GS** ribbons (Figure 1, Table 1). Benzene, which has a slightly larger molecular volume ($V_g = 79$ Å$^3$), templates the formation of the lower density, more open simple brick architecture, affording **G$_2$BDS**·3(*benzene*). The pillars and guests are isostructural and exhibit herringbone packing, made possible by the ability of the **BDS** pillars to rotate about their C−S bonds. We reported other isostructural combinations, **G$_2$NDS**·3(*naphthalene*), **G$_2$BPDS**·3(*biphenyl*), and **G$_2$ADS**·3(*anthracene*),[8] with similar herringbone pillar−guest packings that mimic the layer motifs in the crystals of their respective pure guests. The pillar−guest organization in **G$_2$BDS**·3(*benzene*), however, approaches that of the herringbone layers in the more densely packed high pressure form of pure benzene rather than its ambient form.[13]

The **G$_2$ADS** host also exhibits bilayer−simple brick isomerism, although with proportionally larger guest molecules. Naphthalene guests are incorporated in the bilayer framework as **G$_2$ADS**·(*naphthalene*), but the larger pyrene promotes the formation of the simple brick **G$_2$ADS**·(*pyrene*). This can be attributed to the large size of the pyrene guests, which cannot be accommodated by the undersized inclusion cavities of the bilayer framework. The pyrene guests are confined within ∼7.5 Å wide channels, perpendicular to the **GS** major ribbon direction and flanked by the **ADS** pillars. **G$_2$BDS**·3(*benzene*) and **G$_2$ADS**·(*pyrene*) illustrate the extraordinary capacity of the simple brick

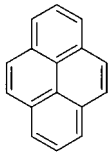

pyrene

architecture to adapt to the steric demands of the guest molecules through puckering of the conformationally flexible **GS** sheet about its major ribbon edges (defined by the interribbon angle $\theta_{IR}$, see Figure 1). Puckering allows the host to significantly adjust its inclusion cavity volume, $V_{inc}$, and "shrink-wrap" about the guests. This, combined with rotation of the pillars about their C−S bonds, provides the host framework with a route to optimized host−guest interactions, similar to behavior described

(11) Molecular volume calculations were performed using MSI Cerius$^2$ v.3.5. $V_g$ values are obtained using a Connolly (van der Waals) surface model with a probe radius of zero and a dot density of 100 Å$^{-1}$. These values tend to be systematically lower, by up to ca. 6%, than those determined by traditional means (see Kitaigorodski, A. I. *Molecular Crystals and Molecules*; Academic Press: New York, 1973; pp. 18−21). $V_{inc}$ values are obtained by determining the "available volume" (probe radius = 0.5 Å, grid spacing of "fine") in the unit cell after removal of guests and normalizing to one host formula unit. $V_{host}$ values are calculated by subtracting the "available volume" from the unit cell volume and normalizing to one host formula unit. These values are consistent, to within 5 Å$^3$, among different inclusion compounds of the same host.

(12) Bilayer host frameworks often exhibit a "shifted ribbon", rather than quasihexagonal, **GS** sheet motif. The shifted-ribbon motif is generated by a translation of adjacent **GS** ribbons by up to one-half of the ribbon repeat distance. This minor structural variation is thought to be a consequence of subtle steric packing forces between the pillars and guests. Because the supramolecular connectivities of the quasihexagonal and shifted-ribbon motif differ, frameworks with different **GS** motifs can be regarded as supramolecular isomers but technically are not architectural isomers. For every pillar that adopts a bilayer framework we have observed at least one example that exhibits the quasihexagonal sheet motif. Thus, the bilayer framework can be regarded as a true architectural isomer of its corresponding brick forms.

(13) The observation of nonambient herringbone packing can be attributed to the structural incompatibility of the **GS** host lattice and the ambient motif. The 2-D herringbone motif of the ambient and high pressure form of benzene have lattice dimensions of 7.44 Å × 6.92 Å (area/benzene molecule = 51.5 Å$^2$) and 7.35 Å × 5.38 Å (area/benzene molecule = 39.5 Å$^2$), respectively. The pillar−guest layers in **G$_2$BDS**·3(*benzene*) exhibit lattices of 7.65 Å × 11.62 Å, corresponding to 7.65 Å × 5.81 Å (area = 44.5 Å$^2$) if the crystallographic symmetry of the layers is ignored. Pillar−guest packing with the ambient density would require a lattice dimension normal to the **GS** ribbon of 2 × 6.92 Å = 13.84 Å, which exceeds the width of two **GS** ribbons (2 Å × 6.5 Å = 13.0 Å). Equivalently, the area required by the ambient phase exceeds the available area of 48.75 Å$^2$ in a framework having a flat quasihexagonal **GS** sheet. The actual area occupied by the benzene pillars and guests is less than this ideal value owing to puckering of the **GS** host, which effectively exerts an internal lattice pressure that enforces the denser packing of benzene guests and benzene pillar fragments.

**Table 1.** Summary of Crystallographic Data for Reported Compounds

| compound | **G$_2$BDS**·(thf) | **G$_2$BDS**·3(benzene) | **G$_2$BDS**·2(*p*−xylene) | **G$_2$BDS**·2(*o*−xylene) | **G$_2$BDS**·2(naphthalene) | **G$_2$NDS**·(benzene) | **G$_2$NDS**·(*p*−xylene) |
|---|---|---|---|---|---|---|---|
| formula | $C_{12}H_{24}N_6O_7S_2$ | $C_{26}H_{34}N_6O_6S_2$ | $C_{24}H_{36}N_6O_7S_2$ | $C_{24}H_{36}N_6O_6S_2$ | $C_{12}H_{24}N_6O_7S_2$ | $C_{18}H_{24}N_6O_6S_2$ | $C_{20}H_{28}N_6O_6S_2$ |
| formula wt | 428.49 | 590.72 | 568.70 | 568.70 | 612.72 | 484.56 | 512.60 |
| crystal system | monoclinic | monoclinic | orthorhombic | orthorhombic | orthorhombic | triclinic | triclinic |
| space group | *Cmcm* | $P2_1/n$ | *Pbca* | *Pbca* | *Pbca* | $P\bar{1}$ | $P\bar{1}$ |
| color | colorless | colorless | colorless | colorless | colorless | colorless | colorless |
| *a* (Å) | 7.5299(6) | 7.6465(6) | 13.4285(9) | 13.1459(8) | 13.360(1) | 6.2166(3) | 7.2609(9) |
| *b* (Å) | 12.465(1) | 11.6218(9) | 12.5989(9) | 12.4292(8) | 12.647(1) | 7.1847(4) | 7.4075(9) |
| *c* (Å) | 21.430(2) | 17.625(2) | 17.785(2) | 18.882(2) | 18.168(2) | 13.1213(7) | 13.154(2) |
| α (deg) | 90 | 90 | 90 | 90 | 90 | 74.725(1) | 89.189(2) |
| *β* (deg) | 90 | 96.211(1) | 90 | 90 | 90 | 83.331(1) | 77.186(2) |
| *γ* (deg) | 90 | 90 | 90 | 90 | 90 | 85.826(1) | 62.193(2) |
| *V* (Å$^3$) | 2011.4(3) | 1557.1(2) | 3008.9(4) | 3085.3(3) | 3069.8(4) | 560.98(5) | 560.98(2) |
| temp (K) | 173(2) | 173(2) | 173(2) | 173(2) | 173(2) | 173(2) | 173(2) |
| *Z* | 4 | 2 | 2 | 2 | 2 | 1 | 1 |
| $R_1$ [$I > 2\sigma(I)$] | 0.0318 | 0.0418 | 0.0344 | 0.0424 | 0.0326 | 0.0338 | 0.0343 |
| $wR_2$ [$I > 2\sigma(I)$] | 0.0875 | 0.1130 | 0.0971 | 0.1201 | 0.0795 | 0.0882 | 0.0941 |
| G.O.F. | 1.097 | 1.19 | 1.06 | 1.081 | 1.026 | 1.037 | 1.075 |

| compound | **G$_2$NDS**·3(o−xylene) | **G$_2$NDS**·2(1−MN) | **G$_2$NDS**·2(pyrene) | **G$_2$BPDS**·2(perylene) | **G$_2$ADS**·(*p*−xylene) | **G$_2$ADS**·(*o*−xylene) | **G$_2$ADS**·(naphthalene) |
|---|---|---|---|---|---|---|---|
| formula | $C_{36}H_{48}N_6O_6S_2$ | $C_{34}H_{38}N_6O_6S_2$ | $C_{44}H_{38}N_6O_6S_2$ | $C_{54}H_{44}N_6O_6S_2$ | $C_{24}H_{30}N_6O_6S_2$ | $C_{24}H_{30}N_6O_6S_2$ | $C_{26}H_{28}N_6O_6S_2$ |
| formula wt | 724.92 | 690.82 | 810.92 | 937.08 | 562.66 | 562.66 | 584.66 |
| crystal system | monoclinic | orthorhombic | orthorhombic | orthorhombic | triclinic | triclinic | triclinic |
| space group | $P2_1/n$ | *Pbca* | *Pbca* | *Pbca* | $P\bar{1}$ | $P\bar{1}$ | $P\bar{1}$ |
| color | colorless | colorless | colorless | orange | pale yellow | pale yellow | pale yellow |
| *a* (Å) | 7.5334(6) | 13.3756(3) | 13.4471(4) | 13.6864(7) | 6.2024(4) | 6.2001(5) | 6.2127(6) |
| *b* (Å) | 12.2651(9) | 12.4586(3) | 12.1155(4) | 12.4544(7) | 7.1901(5) | 7.3015(6) | 7.19775(7) |
| *c* (Å) | 20.621(2) | 22.3040(5) | 23.9856(7) | 26.473(2) | 15.184(1) | 15.145(2) | 15.372(2) |
| α (deg) | 90 | 90 | 90 | 90 | 80.859(1) | 103.134(2) | 78.105(2) |
| *β* (deg) | 96.645(1) | 90 | 90 | 90 | 82.235(1) | 94.777(1) | 81.376(2) |
| *γ* (deg) | 90 | 90 | 90 | 90 | 85.208(1) | 92.607(2) | 87.493(2) |
| *V* (Å$^3$) | 1892.5(3) | 3716.8(2) | 3907.7(2) | 4512.4(4) | 661.1(1) | 663.0(1) | 664.9(1) |
| temp (K) | 173(2) | 173(2) | 173(2) | 173(2) | 173(2) | 173(2) | 173(2) |
| *Z* | 2 | 4 | 4 | 4 | 1 | 1 | 1 |
| $R_1$ [$I > 2\sigma(I)$] | 0.0403 | 0.0568 | 0.0371 | 0.0422 | 0.0363 | 0.0381 | 0.0386 |
| $wR_2$ [$I > 2\sigma(I)$] | 0.1110 | 0.1569 | 0.0869 | 0.1020 | 0.0964 | 0.1008 | 0.1091 |
| G.O.F. | 1.022 | 1.047 | 1.019 | 1.049 | 1.070 | 1.064 | 1.090 |

| compound | **G$_2$ADS**·(pyrene) | **G$_2$ADS**·3(biphenyl) | **G$_2$ADS**·2(perylene) | **G$_2$ODS** | **G$_2$ODS**·(hexane) | **G$_2$PEDS**·(toluene) | **G$_2$PEDS**·3(acetonitrile) |
|---|---|---|---|---|---|---|---|
| formula | $C_{32}H_{30}N_6O_6S_2$ | $C_{52}H_{50}N_6O_6S_2$ | $C_{56}H_{44}N_6O_6S_2$ | $C_{10}H_{28}N_6O_6S_2$ | $C_{16}H_{42}N_6O_6S_2$ | $C_{21}H_{28}N_6O_7S_2$ | $C_{20}H_{29}N_9O_7S_2$ |
| formula wt | 658.74 | 919.10 | 961.10 | 392.15 | 464.24 | 540.62 | 571.64 |
| crystal system | monoclinic | monoclinic | orthorhombic | orthorhombic | orthorhombic | triclinic | orthorhombic |
| space group | $P2_1/n$ | *Pn* | *Pbca* | $Pna2_1$ | *Pnma* | $P\bar{1}$ | $P2_12_12_1$ |
| color | pale yellow | pale yellow | orange | colorless | colorless | colorless | colorless |
| *a* (Å) | 7.447(1) | 7.4697(8) | 13.789(2) | 12.658(2) | 14.426(1) | 7.5011(9) | 7.4659(4) |
| *b* (Å) | 9.873(2) | 26.627(3) | 12.303(1) | 42.116(4) | 22.438(2) | 12.092(2) | 13.7874(8) |
| *c* (Å) | 20.756(3) | 11.836(2) | 26.784(2) | 11.596(1) | 7.4303(6) | 29.989(5) | 29.084(2) |
| α (deg) | 90 | 90 | 90 | 90 | 90 | 84.585(1) | 90 |
| *β* (deg) | 94.601(3) | 92.100(2) | 90 | 90 | 90 | 86.477(9) | 90 |
| *γ* (deg) | 90 | 90 | 90 | 90 | 90 | 89.23(1) | 90 |
| *V* (Å$^3$) | 1521.2(3) | 2352.5(4) | 4544.0(7) | 6182(1) | 2405.2(3) | 2702.7(6) | 2993.8(3) |
| temp (K) | 173(2) | 173(2) | 173(2) | 173(2) | 173(2) | 173(2) | 173(2) |
| *Z* | 2 | 2 | 2 | 12 | 4 | 2 | 4 |
| $R_1$ [$I > 2\sigma(I)$] | 0.0413 | 0.0457 | 0.0439 | 0.0541 | 0.0666 | 0.0511 | 0.0564 |
| $wR_2$ [$I > 2\sigma(I)$] | 0.0967 | 0.0702 | 0.0898 | 0.1310 | 0.2163 | 0.01035 | 0.01453 |
| G.O.F. | 0.905 | 0.812 | 1.06 | 1.018 | 1.075 | 0.877 | 1.098 |

| compound | **G$_2$PEDS**·(mesitylene)·(MeOH) | **G$_2$MDS**·(acetone)·(MeOH) | **G$_2$MDBDS**·2(thf) |
|---|---|---|---|
| formula | $C_{24}H_{36}N_6O_8S_2$ | $C_{15}H_{32}N_6O_8S_2$ | $C_{19}H_{38}N_6O_9S_2$ |
| formula wt | 600.71 | 488.59 | 558.68 |
| crystal system | orthorhombic | orthorhombic | orthorhombic |
| space group | $P2_12_12_1$ | $Cmc2_1$ | *Pnma* |
| color | colorless | colorless | colorless |
| *a* (Å) | 7.5839(4) | 7.501(1) | 21.1037(8) |
| *b* (Å) | 14.2280(8) | 20.576(3) | 7.5867(4) |
| *c* (Å) | 27.748(2) | 15.796(2) | 19.3182(8) |
| α (deg) | 90 | 90 | 90 |
| *β* (deg) | 90 | 90 | 90 |
| *γ* (°) | 90 | 90 | 90 |
| *V* (Å$^3$) | 2994.2(3) | 2438.1(6) | 3093.2(2) |
| temp (K) | 173(2) | 173(2) | 173(2) |
| *Z* | 4 | 4 | 4 |
| $R_1$ [$I > 2\sigma(I)$] | 0.0408 | 0.0317 | 0.0967 |
| $wR_2$ [$I > 2\sigma(I)$] | 0.1044 | 0.0823 | 0.2432 |
| G.O.F. | 1.050 | 1.098 | 1.012 |

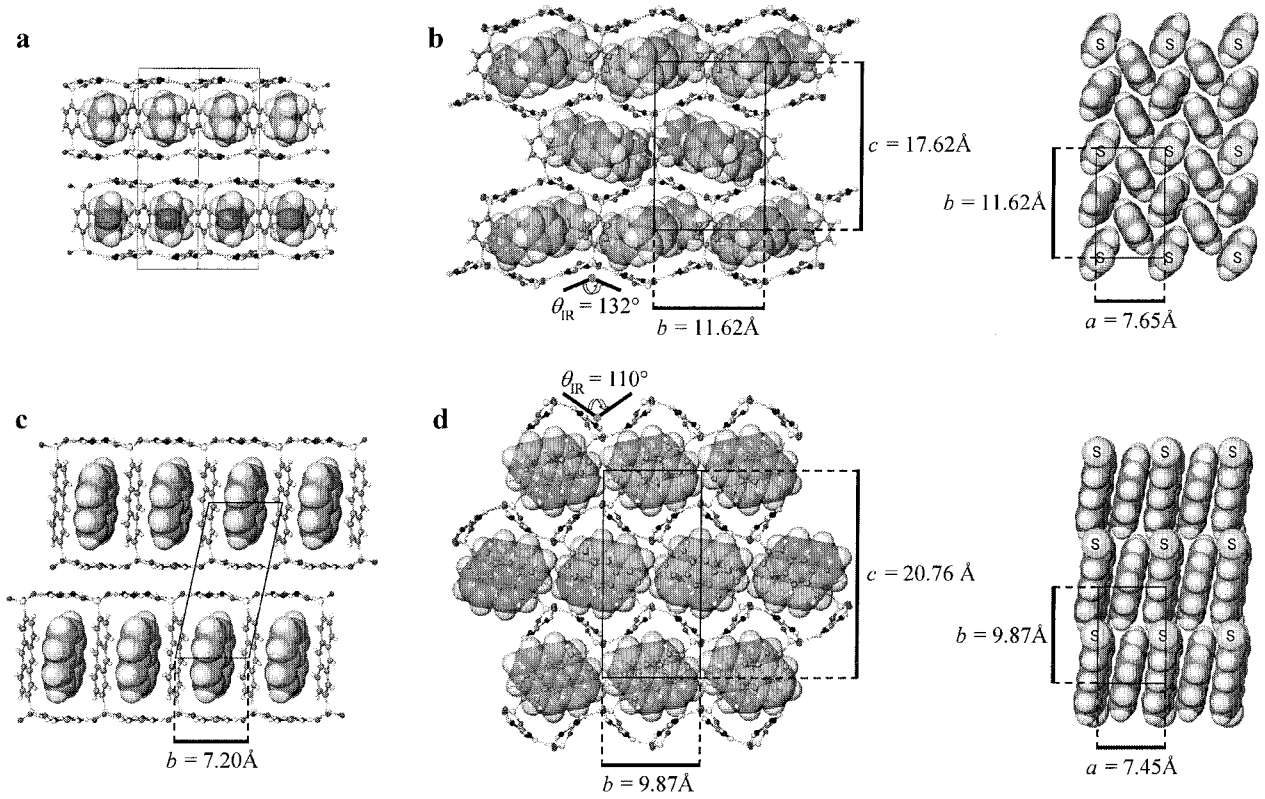


**Figure 1.** **GS** inclusion compounds exemplifying the bilayer−simple brick isomerism. (a) Bilayer **G₂BDS**·(*tetrahydrofuran*) as viewed down [110], (b) simple brick **G₂BDS**·3(*benzene*), (c) bilayer **G₂ADS**·(*naphthalene*), (d) simple brick **G₂ADS**·(*pyrene*). The host frameworks are drawn as wireframe and the guests as space-filling. The right-hand panels in (b) and (d) depict the top-down view of the pillar−guest packing within the gallery regions of the brick frameworks. The guanidinium ions and oxygen atoms of the sulfonates in the **GS** sheets have been removed for clarity, and the major ribbons are parallel to the *a* axes. $\theta_{IR}$ represents the interribbon puckering angle.

above for **G₂BDS**·3(*benzene*). This remarkable flexibility is typical of simple brick frameworks and allows inclusion stoichiometries ranging from 1:1 to 1:4, the higher guest occupancies associated with significantly less puckering. We recently demonstrated that the maximum inclusion cavity volume, $V_{inc}^{max}$, available in a simple brick host with a given pillar could be determined through the use of master curves, based on an analytic function, which describe the dependence of $V_{inc}$ on the $\theta_{IR}$, the pillar length, and the intrinsic molecular volume of the host, $V_{host}$.[14] For a given pillar, the pillar length and $V_{host}$ are constants such that $V_{inc}$ is solely dependent upon $\theta_{IR}$.

The bilayer and simple brick **GS** sheets can be distinguished by their "projection topologies," which describe the "up/down" arrangement of the pillars projecting from the sulfonate nodes on the **GS** sheets. For convenience, each **GS** sheet can be described as consisting of "major" (*M*) and "minor" (*m*) **GS** ribbons. The pillars in the bilayer frameworks project either all "up" or all "down" from each sheet as depicted by topology **I** in Figure 2. In contrast, in the simple brick architecture the pillars along each major ribbon project to the same side of the sheet, but the pillars on adjacent ribbons project to opposite sides, generating topology **II**. Consequently, along the major ribbons the pillars project either all up or all down, but alternate ...up,down,up,down... along the "minor" ribbons. These and more complicated projection topologies can be described by a formalism that reveals the symmetry constraints on the projection sequences for the various up/down combinations and facilitates the conjecture of possible continuous brick framework isomers.[15]

The **G₂BDS**, **G₂NDS**, **G₂BPDS**, and **G₂ADS** compounds establish the generality of bilayer−simple brick architectural isomerism and the role of steric complementarity. The projection topologies **I** and **II** are ubiquitous in the **GS** inclusion compounds and guanidinium organo*mono*sulfonates.[16] The latter have lamellar "interdigitated bilayer" and "continuously interdigitated" architectures that mirror the bilayer and simple brick inclusion architectures, respectively. The projection topology in our previously observed **G**[1-butanesulfonate],[16a] however, is a singular exception, adopting a "zigzag" topology (**III**) in which the projection of the organosulfonate residues alternate ...up, down... along the major ribbons and ...up, up, down, down... along the minor ribbons. Given the monosulfonate−disulfonate homology demonstrated for the bilayer and brick architectures, this prompted us to explore whether the zigzag topology could be reproduced in **G₂**[organodisulfonate] frameworks.

We reported previously that **G₂**[1,4-butanedisulfonate]·2(*acetonitrile*) crystallizes in the bilayer framework with topology **I**. In contrast, **G₂ODS**, crystallized from methanol, forms a guest-free continuous zigzag brick framework, a new brick architecture with a projection topology (**III**) identical to that in **G**[1-butanesulfonate] (Figure 3). It may seem surprising that this framework exists without the inclusion of guests. The *gauche* conformations at the terminal C−C−C−S segments ($\tau = 89°$), and *anti* conformations within the internal $C_6$ segment, however, result in an antiparallel orientation of the sulfonate groups that allows the pillars to bridge opposing **GS** sheets,

(14) The values of $V_{inc}$ can be calculated from $V_{inc} = (V_{cell} - 2V_{host})/2$, wherein $V_{inc}$ is normalized to one host formula unit and $V_{cell}$ is given by $V_{cell} = [7.5]\cdot[13.0 \sin(\theta_{IR}/2)]\cdot[13.0 \cos(\theta_{IR}/2) + 2l]$ Å$^3$ where *l* is the pillar length, as measured by the S−S separation within the pillar. See ref 6.

but with the long axes of the pillars nearly parallel to the **GS** sheets. This orientation affords an average intersheet spacing of $c/2 = 5.80$ Å, substantially less than one may expect on the basis of the length of the **ODS** pillar. This structure results in a packing fraction (0.65) that is on the low end of values typical of molecular crystals. This suggests that the adoption of the *gauche*−(*anti*)$_5$−*gauche* pillar conformation and the resulting interpillar packing is a reasonable low-energy alternative to inclusion (the energy of the *gauche* conformation is ∼1 kcal/mol higher than that of the *anti*). It is important to note that all *anti* **ODS** pillars oriented perpendicular to the **GS** sheets could, in principle, produce an even lower-density zigzag brick architecture (or possibly other architectures), capable of guest inclusion. It is reasonable to suggest, however, that open zigzag brick frameworks are more likely for rigid pillars.

Indeed, the zigzag brick architecture is observed in the 1:2 inclusion compounds **G$_2$BDS**·2(*p-xylene*), **G$_2$BDS**·2(*o-xylene*), and **G$_2$BDS**·2(*naphthalene*) (Figure 4). The guests effectively serve as templates for this architecture and are confined as face-to-face dimers within the inclusion cavities generated by the zigzag arrangement of pillars between the **GS** sheets. The sheets are puckered like an egg carton rather than the pleated puckering exhibited by the simple brick form. The dimers exhibit edge-to-face ordering with the **BDS** pillars and with arene dimers in neighboring inclusion cavities (the intermolecular dihedral angles associated with this packing are provided in Figure 4). It is interesting to note that naphthalene, *p*-xylene, and *o*-xylene do not adopt these face-to-face geometries within their native crystal structures.[17−19]

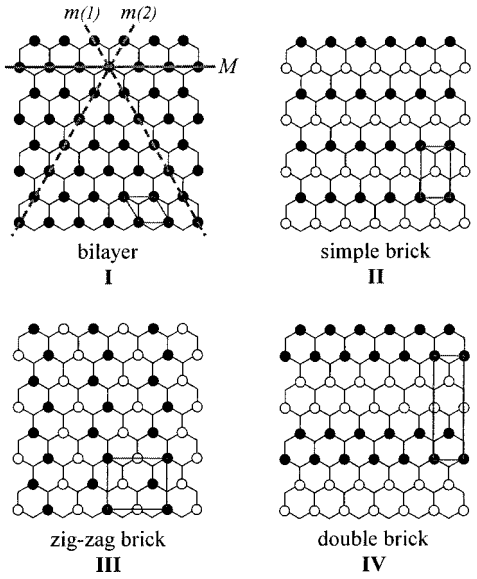


**Figure 2.** Top-view representations of the projection topologies of the organodisulfonate pillars on each individual **GS** sheet in the four architectural isomers that have been observed in **GS** hosts. Filled and open circles depict pillars projecting above and below the sheet, respectively. The "up" pillars connect to the adjacent **GS** sheet above the plane of the page and the "down" pillars connect to the adjacent **GS** sheet below the plane of the page. The guanidinium ions sit on the undecorated nodes of the quasihexagonal tiling. The solid and dashed lines represent the major ribbons, *M*, and the minor ribbons, *m(1)* and *m(2)*, respectively. The parallelograms depict the translational repeat unit of each sheet.

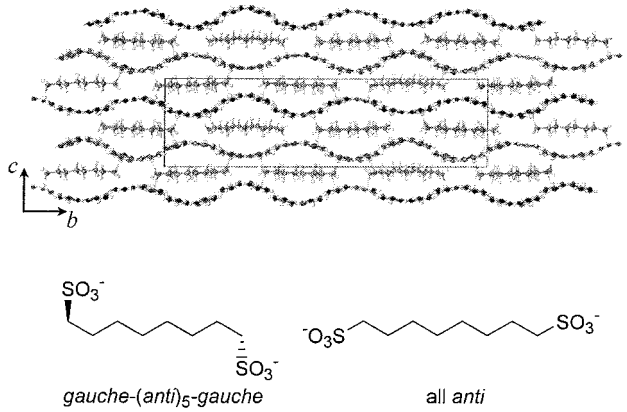


**Figure 3.** (a) Zigzag brick, guest-free **G$_2$ODS**. The projection topology of the **ODS** pillars is identical to that adopted by the monosulfonate salt **G**[1-butanesulfonate].

The **G$_2$NDS** host framework exhibits similar trends with respect to steric complementarity and architectural isomerism, but with proportionally larger guest molecules. The longer **NDS** pillar provides more inclusion volume compared to **BDS**. Thus, benzene and *p*-xylene, which template simple brick and zigzag brick architectures, respectively, for **G$_2$BDS**, can be accommodated in the bilayer framework of **G$_2$NDS**, affording **G$_2$NDS**·(*benzene*)[20] and **G$_2$NDS**·(*p*-xylene). The apparent inability of the larger naphthalene guest to fit within the undersized inclusion cavities of the **G$_2$NDS** bilayer framework allows it to template the formation of the simple brick architecture in **G$_2$NDS**·3(*naphthalene*). We presume that this architecture is also favored by the achievement of near-ideal herringbone pillar−guest packing. Interestingly, **G$_2$NDS**·3(*o*-xylene) adopts a simple brick

(15) The topologies for the bilayer and continuous architectures can be described by a formalism, $M(n)^{u(n)}_{d(n)}m(1)^{u(1)}_{d(1)}m(2)^{u(2)}_{d(2)}$, where *M(n)*, *m(1)* and *m(2)* denote *n* number of major and two minor ribbons, respectively, and *u* and *d* are indices that describe the projection sequence of the pillars on the respective ribbons. The number of *M(n)* terms required for an unambiguous description the projection topology of a given sheet is equal to the number of rows that define a unit translation in the **GS** sheet along the direction perpendicular to the major ribbon. The major ribbons are chosen, by convention, as those that describe the repeating sequence normal to these ribbons with the least number of *M(n)* terms. The full notations for projection topologies of the bilayer (**I**) and simple brick (**II**) isomers are $M^1_0\,M^1_0$ and $M^1_0\,M^0_1m(1)^1_1m(2)^1_1$, respectively, although the shorter descriptions $M^1_0\,M^1_0$ and $M^1_0\,M^0_1$ define these two isomers unambiguously. The toplogies of adjacent sheets are related to each other by reflection. The projection topologies of the zigzag (**III**) and double-brick isomer (**IV**) can be described in a similar manner using this formalism. Architectures with identical numbers of up and down pillars on each sheet, like the simple brick form, can be described universally as

$$M(n)^{u(n)}_{d(n)}\,m(1)^{u^{i_1},u^{i_2},u^{i_3}\ldots}_{d^{i_1},d^{i_2},d^{i_3}\ldots}\,m(2)^{u^{i_1},u^{i_2},u^{i_3}\ldots}_{d^{i_1},d^{i_2},d^{i_3}\ldots}$$

where the *i, j, k* terms need not be identical for the different ribbons but

$$\sum_{k=1,2,3,\ldots}^{u(1)} i_k = \sum_{k=1,2,3,\ldots}^{u(2)} i_k = \sum_n u(n) \quad \text{and}$$

$$\sum_{k=1,2,3,\ldots}^{d(1)} i_k = \sum_{k=1,2,3,\ldots}^{d(2)} i_k = \sum_n d(n).$$

These summation rules are useful because they establish the repeat interval of the projection sequence, which becomes more difficult to assign as the sequence intervals contain more terms in more complex topologies.

(16) (a) Russell, V. A.; Etter M. C.; Ward, M. D. *J. Am. Chem. Soc*. **1994**, *116*, 1941. (b) Russell, V. A.; Etter M. C.; Ward, M. D. *Chem. Mater*. **1994**, *6*, 1206. (c) Russell, V. A.; Ward, M. D. *Acta Crystallogr*. **1996**, *B52*, 209. (d) Russell. V. A.; Ward, M. D. *J. Mater. Chem.* **1997**, *7*, 1123. (e) Russell, V. A.; Ward, M. D. *New J. Chem.* **1998**, 149.

(17) Biswas *Indian J. Phys*. **1960**, *34*, 263.

(18) van Koningsveld, H.; van den Berg, A. J.; Jansen, J. C.; de Goede, R. *Acta Crystallogr., Sect. B* **1986**, *42*, 491.

(19) Abrahams, S. C.; Robertson, J. M.; White, J. G. *Acta Crystallogr*. **1949**, *2*, 233.

(20) The host framework in **G$_2$NDS**·(*benzene*) exhibits the shifted-ribbon motif.

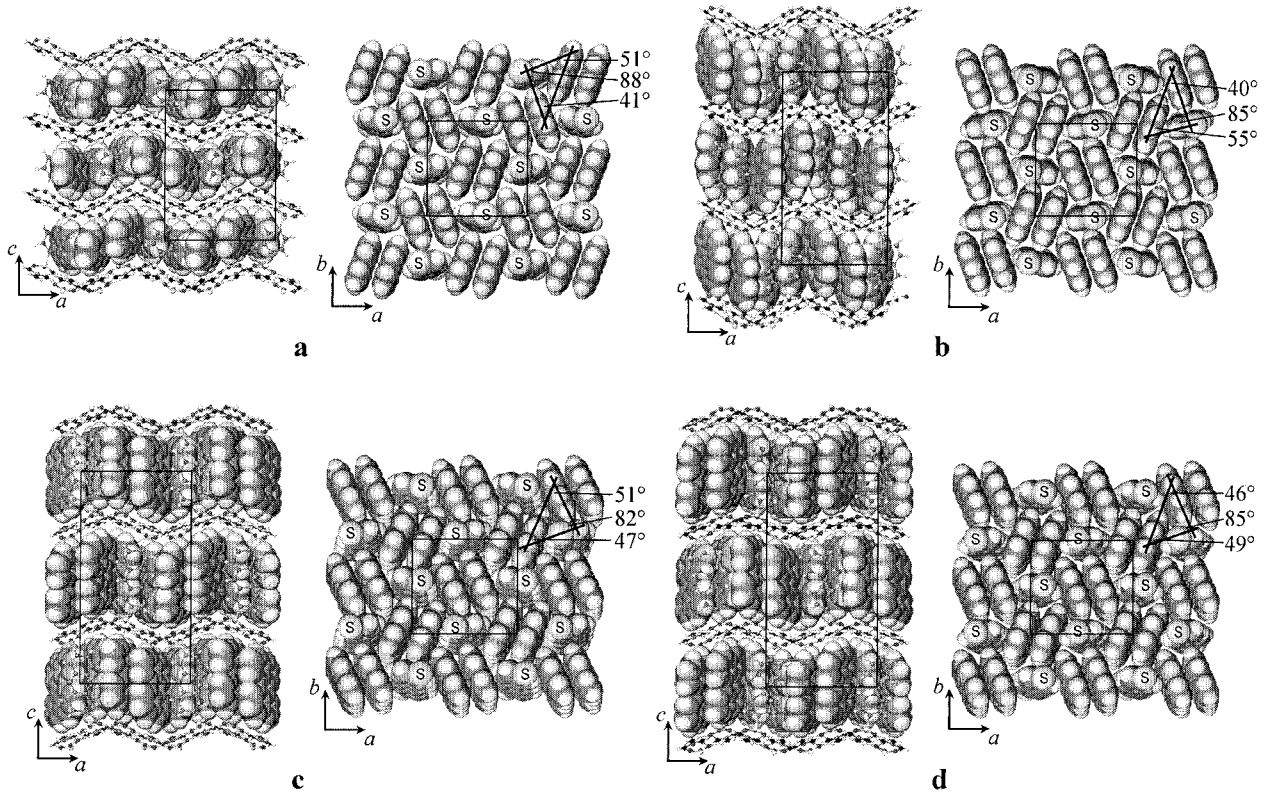


**Figure 4.** Zigzag brick inclusion compounds: (a) **G₂BDS**·*2*(*naphthalene*). (b) **G₂NDS**·2(*pyrene*). (c) **G₂ADS**·2(*perylene*), and (d) **G₂BPDS**·2(*perylene*). The major ribbons are parallel to the *a* axes.

architecture, illustrating that factors other than simple sterics, such as guest shape, sometimes play an important structure-directing role.

Architectural isomerism for **G₂NDS** can be extended to the zigzag brick by using the larger 1-methylnaphthalene(1−MN) and pyrene guests, which afford **G₂NDS**·2(*1-methylnaphthalene*) and **G₂NDS**·2(*pyrene*). Like the corresponding zigzag brick **G₂BDS** compounds, the guests are situated as face-to-face arene dimers, exhibiting edge-to-face contacts with the four surrounding **NDS** pillars and the guest dimers of adjacent cavities. Notably, the local structure of the pyrene dimers is essentially identical to that observed for the dimers in single crystals of pure pyrene, with identical interplanar separations (3.43 Å) and offset geometry.[21] Given the observation of non-native face-to-face dimers of naphthalene, *o*-xylene and *p*-xylene in the zigzag brick **G₂BDS** compounds, we surmise that the pyrene dimers in **G₂NDS**·2(*pyrene*) reflect an optimization of guest−guest and host−guest interactions rather than a strong structure-directing role for the pyrene dimers.

The steric origins of architectural isomerism are also evident in **G₂BPDS** and **G₂ADS** inclusion compounds. As one would expect on the basis of the size and length of the pillars, the inclusion compounds of *p*-xylene and *o*-xylene adopt the bilayer architecture with a 1:1 stoichiometry. Although naphthalene is large enough to template the formation of a simple brick architecture for **G₂NDS**, it is accommodated by the bilayer frameworks of **G₂BPDS** and **G₂ADS** as 1:1 inclusion compounds. The simple brick architectures of **G₂BPDS** and **G₂ADS** can be formed, however, with rather large guests, as illustrated by **G₂BPDS**·3(*biphenyl*), **G₂ADS**·3(*biphenyl*), and the aforementioned highly puckered 1:1 compound, **G₂ADS**·(*pyrene*). Despite numerous attempts, we have not yet been able to prepare the corresponding pyrene inclusion compound of **G₂BPDS**. In a trend that parallels the isomerism observed for the **G₂BDS** and **G₂NDS** hosts, a further increase in guest size to perylene affords the zigzag brick architectures in **G₂BPDS**·2(*perylene*) and **G₂ADS**·2(*perylene*). As with the pyrene dimers in the zigzag **G₂NDS**, the perylene dimers in these compounds adopt a face-to-face configuration, with an interplanar separation of 3.42 Å, that is identical to that observed in α-perylene.[22] We have also demonstrated that the **G₂ABDS** host, with the even longer **ABDS** pillar, can accommodate still larger guest molecules (e.g., 1,4-divinylbenzene) in a bilayer framework.[4d]

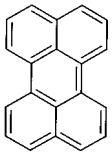
perylene

As mentioned above, we recently established that, for a given simple brick host, $V_{inc}$ depends on the interribbon puckering angle, $\theta_{IR}$, according to a simple analytic function.[14] Notably, $V_{inc}^{max}$, the overall maximum achievable inclusion cavity volume (normalized to host stoichiometry, *Z*, Table 1), *is not achieved when the GS sheets are flat*. The observed $V_{inc}$ values in **G₂BDS**·3(benzene) ($\theta_{IR} = 132°$), **G₂NDS**·3(*naphthalene*) ($\theta_{IR} = 133°$), **G₂BPDS**·3(*biphenyl*) ($\theta_{IR} = 130°$), and **G₂ADS**·3(*biphenyl*) ($\theta_{IR} = 130°$) are near their respective $V_{inc}^{max}$ predicted by this function. In contrast, the highly puckered simple brick compound **G₂ADS**·(pyrene) ($\theta_{IR} = 110°$) has a $V_{inc}$ that is significantly smaller than $V_{inc}^{max}$ for this host.

We surmise that the egg-carton puckering of the zigzag brick structures also serves to increase $V_{inc}$, beyond what would be

(21) Camerman, A.; Trotter, J. *Acta Crystallogr.* **1965**, *18*, 636.

(22) Camerman, A.; Trotter, J. *Proc. R. Soc. London, Ser. A* **1964**, *279*, 129.

**Table 2.** Selected Structural Features for **GS** Inclusion Compounds Exhibiting the Bilayer, Simple Brick, and Zigzag Brick Architectures

| host | *n*guest | architectural isomer | $V_g$ [a] (Å3) | $nV_g$ (Å$^3$) | $V_{inc}$ [a] (Å3) | $V_{cell}$ [b] (Å3) |
|---|---|---|---|---|---|---|
| **$G_2$BDS** | tetrahydrofuran | bilayer | 73 | 73 | 235 | 503 |
| $V_{host}$ [a] = 268 Å$^3$ | 3(benzene) | simple brick | 79 | 237 | 505 | 778 |
| | 2(*p*-xylene) | zigzag brick | 112 | 224 | 484 | 752 |
| | 2(*o*-xylene) | zigzag brick | 112 | 224 | 503 | 771 |
| | 2(naphthalene) | zigzag brick | 122 | 244 | 499 | 767 |
| **$G_2$NDS** | benzene | bilayer | 79 | 79 | 250 | 561 |
| $V_{host}$ [a] = 311 Å$^3$ | *p*-xylene | bilayer | 112 | 112 | 296 | 607 |
| | 3(*o*-xylene) | simple brick | 112 | 336 | 635 | 946 |
| | 3(naphthalene)[c] | simple brick | 122 | 366 | 683 | 994 |
| | 2(1-methylnaphthalene) | zigzag brick | 139 | 278 | 618 | 929 |
| | 2(pyrene) | zigzag brick | 181 | 362 | 666 | 977 |
| **$G_2$BPDS** | *p*-xylene[d] | bilayer | 112 | 112 | 303 | 638 |
| $V_{host}$ [a] = 335 Å$^3$ | *o*-xylene[d] | bilayer | 112 | 112 | 299 | 634 |
| | naphthalene[e] | bilayer | 122 | 122 | 301 | 636 |
| | 3(biphenyl)[c] | simple brick | 147 | 441 | 823 | 1158 |
| | 2(perylene) | zigzag brick | 224 | 448 | 793 | 1128 |
| **$G_2$ADS** | *p*-xylene | bilayer | 112 | 112 | 307 | 661 |
| $V_{host}$ [a] = 354 Å$^3$ | *o*-xylene | bilayer | 112 | 112 | 309 | 663 |
| | naphthalene | bilayer | 122 | 122 | 311 | 665 |
| | pyrene | simple brick | 181 | 181 | 407 | 761 |
| | 3(biphenyl) | simple brick | 147 | 441 | 822 | 1176 |
| | 2(perylene) | zigzag brick | 224 | 448 | 782 | 1136 |

[a] See ref 11. [b] $V_{cell}$ values are unit cell volumes that have been normalized to one host formula unit. [c] See ref 8. [d] See ref 4b. [e] See ref 5.

provided with a flat sheet, to allow optimization of host−guest packing within the gallery regions, in a manner similar to the simple brick form. The general trends observed for guest templating of the zigzag **$G_2$BDS**, **$G_2$NDS**, **$G_2$BPDS**, and **$G_2$ADS** hosts suggest a size threshold beyond which guests cannot be accommodated within the simple brick form. The simple and zigzag brick isomers, however, differ only with respect to the *connectivity* between the sheets such that the volume occupied by the pillars between the **GS** sheets is identical for these isomers. Consequently, for a given pillar, both architectures possess essentially the same $V_{inc}^{max}$. Indeed, the observed values of $V_{inc}$, as well as $V_{cell}$ (normalized by *Z*, Table 1), for the slightly puckered simple brick and zigzag brick architectures are similar (Table 2). Although the overall $V_{inc}^{max}$ is identical for the two frameworks, the size and *shape* of the individual cavities are different.

The similarity of the $V_{inc}$ values for the simple and zigzag brick is reflected in their 1:3 and 1:2 inclusion stoichiometries, respectively. The incorporation of larger guest molecules in the zigzag brick allows inclusion of only *two* equivalents of guest per host, as compared to *three* smaller guests for the simple brick. The products $nV_g$, where *n* is the number of guest molecules and $V_g$ is the guest volume, are similar for the simple and zigzag brick compounds (Table 2). Although the values of $nV_g$ in Table 2 appear significantly smaller than their corresponding $V_{inc}$ values, they are comparable if packing fraction typical of the **GS** inclusion compounds (∼0.68) is taken into account.[23] This behavior indicates that certain large guests template a projection topology that allows the formation of differently sized and shaped inclusion cavities capable of accommodating these guests, albeit in reduced quantity. The $V_{inc}$ values for the zigzag brick architecture are more uniform than those of the simple brick. This reflects a greater rigidity of the zigzag brick, for which extensive puckering is frustrated by the absence of a 1-D hydrogen-bonding "hinge" that exists in the simple brick. This is manifested in inclusion stoichiometries of these hosts, with only 1:2 observed for the zigzag brick, in contrast to the range (1:1 to 1:4) of stoichiometries observed for the simple brick.

The observation of stoichiometric inclusion reflects the propensity of the **GS** hosts to form *commensurate* inclusion compounds, in contrast to other well-known channel inclusion hosts such as urea and perhydrotriphenylene.[24] This characteristic can be attributed to the conformational softness of the frameworks, the combination of puckering and pillar rotation permitting inclusion with commensurate registry between the host and guests. The availability of the brick frameworks appears to provide an alternative option for the inclusion of guests that, based on their dimensions, would otherwise appear suitable for inclusion in the corresponding bilayer isomer. For example, the length of the short axis of naphthalene is identical to long axis of benzene, and the lengths of the short axes of pyrene and perylene are identical to the long axis of naphthalene. The benzene and naphthalene guests in the bilayer compounds **$G_2$NDS·**(*benzene*), **$G_2$BPDS·**(*naphthalene*), and **$G_2$ADS·**(*naphthalene*) are oriented with their long axes parallel to the pillar axes. This would suggest that bilayer structures could be observed for naphthalene in **$G_2$NDS**, and pyrene and perylene in **$G_2$BPDS** and **$G_2$ADS** if the guests were properly oriented. Instead, we observe commensurate *brick* architectures in **$G_2$NDS·**3(*naphthalene*), **$G_2$BPDS·**2(*perylene*), **$G_2$ADS·**(*pyrene*) and **$G_2$ADS·**2(*perylene*). This argues that commensurate inclusion of these guests in the bilayer frameworks is difficult.

The systematic and rather predictable behavior exhibited by these hosts illustrates their extraordinary adaptability to differently sized and shaped guests. The guests effectively serve as templates, generating their respective frameworks through a type of "molecular imprinting," reminiscent of the structure-directing influence of molecular templates during the synthesis of microporous silica and polymers.[25−28] We note that topologies

(23) The packing fraction (PF) for each inclusion compound can be calculated by PF = $(V_{host} + nV_g)/V_{cell}$. The values obtained in this way tend to be slightly low, reflecting a systematic error in the reported $V_g$ values.[11]

(24) (a)Hollingsworth, M. E.; Brown, M. E.; Hillier, A. C.; Santasiero, B. D.; Chaney, J. D. *Science* **1996**, *273*, 1355. Brown, M. E.; Chaney, J. D.; Santarsiero, B. D.; Hollingsworth, M. D. *Chem. Mater.* **1996**, *8*, 1588. Hoss, R.; Koenig, O.; Kramer-Hoss, V.; Berger, U.; Rogin, P.; Hulliger, J. *Angew. Chem., Int. Ed. Engl.* **1996**, *35*, 1664. Konig, O.; Burgi, H.-B.; Armbruster, Th.; Hulliger, J.; Weber, Th. *J. Am. Chem. Soc.* **1997**, *119*, 1062. (b) Quintel, A.; Hulliger, J.; Wubbenhorst, M. *J. Phys. Chem. B* **1998**, *102*, 4277. (c) Harris, K. D. M. *Chem. Soc. Rev.* **1997**, *26*, 279.

(25) Katz, A.; Davis, M. E. *Nature* **2000**, *403*, 286.

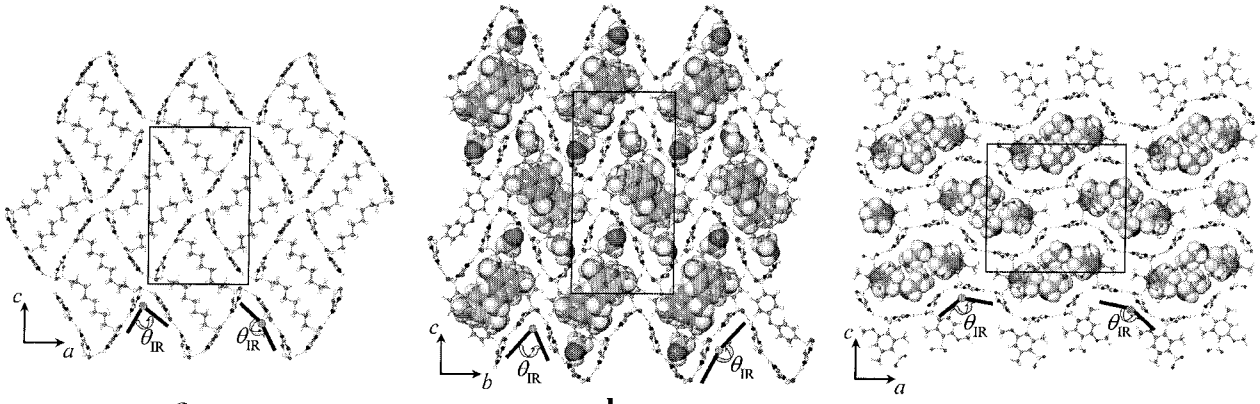


**Figure 5.** Double-brick inclusion compounds: (a) **$G_2$ODS**·(*hexane*) ($\theta_{IR}$ = 77°, 156°). The disordered hexane guest molecules have been removed for clarity. (b) **$G_2$PEDS**·(*mesitylene*)·(*methanol*) ($\theta_{IR}$ = 70°, 162°). (c) **$G_2$** (**MDBDS**)·2(*tetrahydrofuran*) ($\theta_{IR}$ = 121°, 148°). The major ribbons are normal to the plane of the page.

**I**−**IV** have analogues in solid-state inorganic chemistry, specifically the patterns of interstitial cations between cubic close packed layers of anions.[29] In this respect, the locations of the pillars between the **GS** sheets of the bilayer isomer resemble the locations of the metal ions in $MoS_2$. Similarly, the brick, zigzag brick, and double brick isomers have topologies identical to those of $CaCl_2$, α-$PbO_2$, and ξ-$Nb_2C$, respectively. We anticipate, however, that the **GS** hosts can afford more topologies than are possible for the inorganic counterparts, owing to the templating role of the guests, whereby guest molecules force the pillars into topological configurations to accommodate the size and shape of the guests.

**Architectural Isomers with Bent Pillars.** In principle, the 2-D infinite character of the **GS** sheet allows an indefinite number of projection topologies that can produce different continuous brick architectures. The pillars described in the preceding section, including **ODS**, possess antiparallel C−$SO_3^-$ bond vectors such that pillars can be regarded as "straight". We have discovered that "bent" pillars **PEDS** (4,4′-phenyl etherdisulfonate), **MDBDS** (2-methoxy-4,6-dimethyl-1,5-benzenedisulfonate), and **MDS** (mesitylenedisulfonate), as well as **ODS**, can generate a framework isomer with a "double brick" projection topology (**IV**) that can be regarded as a higher order form of the simple brick framework. The pillars in topology **IV** project from the same side of the sheet along adjacent *pairs* of major **GS** ribbons, alternating their projection on the next adjacent pair. This configuration has the potential to create very wide channels (19.5 Å as measured between ribbons, center-to-center), separated by narrower channels having a 6.5 Å width. The formation of such wide channels is precluded, however, by the rather extensive puckering exhibited by the **GS** sheets in these compounds. The puckering involves bending between *pairs* of adjacent **GS** ribbons[30] and needs to be described by two unique $\theta_{IR}$ values. Although presently we have observed the double brick isomer with only these pillars, we cannot identify any obvious structural features that would preclude its formation with others.

Although **$G_2$ODS** forms a guest-free phase when crystallized from methanol, as well as from methanol in the presence of *n*-octane, crystallization from methanol solutions containing *n*-pentane or *n*-hexane affords the double brick inclusion compounds **$G_2$ODS**·(*n*-pentane) and **$G_2$ODS**·(*n*-hexane) (Figure 5). This demonstrates that alkanedisulfonates, as well as arenedisulfonates, are capable of architectural isomerism. The guests and the pillars are highly disordered in these compounds, but the predominant conformation of the pillar is (*anti*)$_5$−*gauche*−*anti*. The ...up,up,down,down... projection sequence, perpendicular to the major **GS** ribbon, can be deduced by tracing the structure along one of the puckered **GS** sheets.

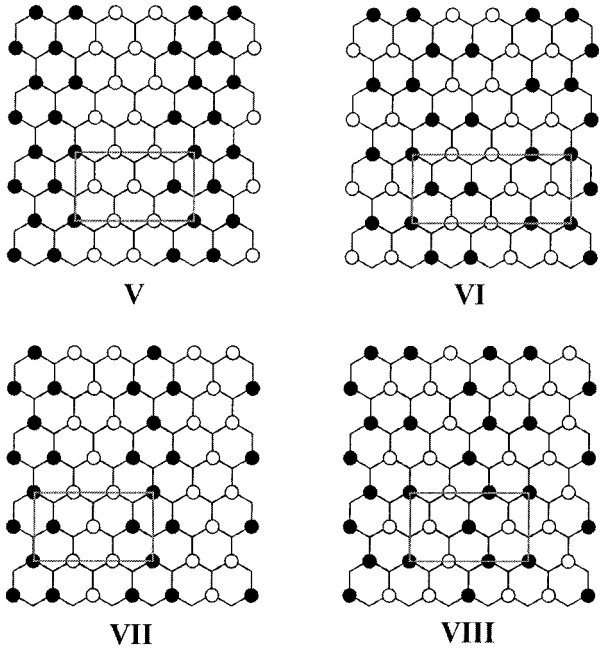


**Figure 6.** **GS** sheet projection topologies of four as yet undiscovered frameworks. The number of up and down projections is identical in each example. These represent a small subset of an unlimited number of combinations.

Architectural isomerism is also observed for **$G_2$PEDS**, with toluene guests promoting the formation of a bilayer framework with the composition **$G_2$PEDS**·(*toluene*). Other guests, however, form inclusion compounds that adopt the double brick structure, as observed for **$G_2$PEDS**·(*mesitylene*)·(*methanol*) and **$G_2$PEDS**·*3*(*acetonitrile*). The guests occupy "pockets" because channels that otherwise would exist along the *b* axis, orthogonal to the **GS** ribbons, are pinched off by the puckering. The double brick framework in **$G_2$**(**MDBDS**)·2(*tetrahydrofuran*) is less corrugated than in the **$G_2$PEDS** compounds, reflecting the shorter pillar

(26) Whitcombe, M. J.; Rodriguez, M. E.; Villar, P.; Vulfson, E. *J. Am. Chem. Soc.* **1995**, *117*, 7105.
(27) Vlatakis, G.; Anderson, L. I.; Müller, R.; Mosbach, K. *Nature* **1993**, *361*, 645.
(28) Shea, K. J. *Trends Polym. Sci.* **1994**, *2*, 166.
(29) Wells, A. F. *Structural Inorganic Chemistry*, 5th ed.; Oxford University Press: Oxford, UK, 1984; pp 167−178.
(30) We have recently observed that the **GS** sheets in **$G_2$PEDS** and **$G_2$MDS** can roll into closed tubes containing an even number of **GS** ribbons; manuscript in preparation.

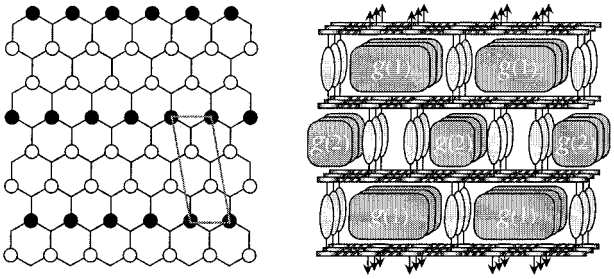

**IX**

**Figure 7.** Projection topology and a side view of a hypothetical inclusion compound in which the number of pillars projecting up from the **GS** sheet is different from the number projecting down. In this example, the projections alternate layer-to-layer as *...n, 2n, n, 2n...*, where *n* is the number of pillars.

length, higher guest occupancy, and protrusion of **MDBDS** methyl groups into the region between adjacent pillars, all of which contribute to space-filling between the **GS** sheets. As with **PEDS**, the **MDBDS** pillars within the ribbon pairs that define the puckering unit have opposed orientations. The observation of these inclusion compounds demonstrates that the lamellar character can be preserved even though the (pillar)C−S(sulfonate) bond vectors are not antiparallel.

**Other Possible Topologies.** The infinite 2-D character of the **GS** sheet suggests an unlimited number of projection topologies and, therefore, an unlimited number of possible continuous brick-like framework isomers. Each isomer will possess a unique inclusion cavity shape as a consequence of the topology-dependent connectivity of the sheets, suggesting that guests must be carefully chosen to template these architectures. We anticipate that projection topology schemes, with accompanying molecular modeling, can serve as a rough guide to choosing guest templates that will promote the formation of new framework architectures. Figure 6 illustrates four examples of as yet unknown topologies (**V**−**VIII**) based on an equal number of "up" and "down" pillars on each sheet. Topology **V** can be regarded as a second-order version of the zigzag topology **IV**, differing with respect to the width of the channels flanked by the pillars. Topology **VI** is a variant of **V**, differing only with respect to the registry of adjacent major ribbons (horizontal). Topology **VII** depicts a configuration in which each major ribbon has twice as many pillars in the "up" projection as "down", or vice-versa, and topology **VIII** is a variant that differs only with respect to the registry of adjacent major ribbons. Overall, the number of pillars projecting from each side of the sheet is the same.

One can also anticipate an unlimited number of other brick isomers in which the number of pillars that project "up" from a given **GS** sheet differ from the number projecting "down." Although such configurations are possible in principle, their syntheses may be difficult because such isomers will possess two distinctly different gallery regions, most likely requiring the simultaneous inclusion of two differently sized and shaped guests. This is illustrated by the hypothetical example with topology **IX** in Figure 7.

**Connectivity Isomerism.** It also is important to consider the possibility of another form of architectural isomerism based on the *connectivity* of the sheets. For example, the bilayer framework of **G$_2$BPDS**·*2*(*methanol*)[4a] exhibits projection topology **I**, but the **BPDS** pillars crisscross when viewed along the ribbon direction, producing a "crisscross bilayer" architectural isomer (bilayer **I-A**, Figure 8). This differs from the 3-D connectivity typically observed for the vast majority of bilayer inclusion compounds (also with projection topology **I**), as exemplified by **G$_2$BDS**·(*tetrahydrofuran*), in which the pillars are eclipsed when viewed along the ribbon direction. Similarly, the connectivity of the sheets in **G$_2$MDS**·(*methanol*)·(*acetone*) differs from that observed in the aforementioned double brick structures, adopting a "V-brick" architecture **IV-A**. The **GS** sheets in **IV-A** have the same projection topology of the double brick architecture, but the sheets are connected together differently. Such connectivity isomers add even more structural variety to the considerable number of possible architectures available through different projection topologies.

## Conclusions

These examples illustrate the remarkable structural diversity of these lamellar **GS** inclusion compounds. The ability to access various architectural isomers with tunable components, based on a common supramolecular building block, removes the constraint of a fixed-sized inclusion environment that limits the choice of guest molecules. Instead, the soft and topologically adaptable **GS** host frameworks can respond to the size and shape requirements of the guest molecules, while the inclusion cavity environment and framework topology can be adjusted by the choice of pillar. We anticipate that carefully designed guest templates can produce new topologies based on the **GS**

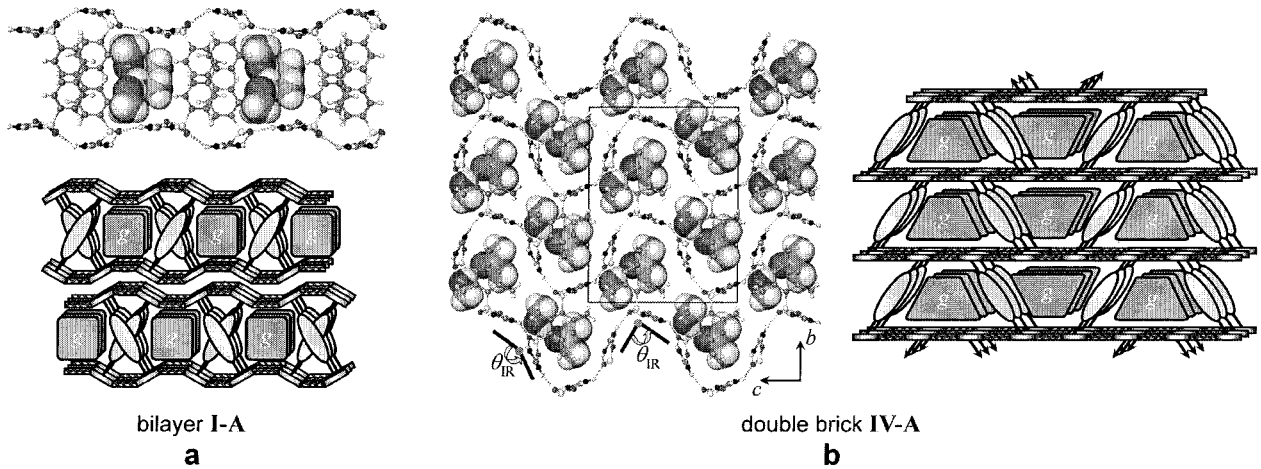


**Figure 8.** (a) The discrete "crisscross bilayer" connectivity isomer I−A in **G$_2$BPDS**·2(*methanol*), as viewed along the major **GS** ribbons. The pillars crisscross when viewed along the **GS** ribbon direction, connecting ribbons that are not directly opposed. (b) The V-brick connectivity isomer IV-A, which has the same projection topology as the double-brick architecture, observed in **G$_2$MDS**·(*methanol*)·(*acetone*).

hydrogen-bonded network. The adaptability of the **GS** hosts endows them with considerable versatility for chemical separations and synthesis of new functional materials for applications such as magnetics and optoelectronics. The **GS** inclusion compounds with pyrene and perylene guests also demonstrate that the spatial organization and aggregation of guest molecules can be controlled, suggesting interesting opportunities for examination of their optical and electronic properties in the confined host matrix. The confinement of guests in these host matrices also suggests possibilities for controlling reactions between a well-defined number of molecules in discrete cavities, for example, dimerization of the guests in the zigzag brick architecture.

## Experimental Section

**Materials and General Procedures.** 4,4-Biphenyldisulfonic acid was purchased from TCI America. The potassium salt of 2,6-anthracene disulfonate,[31] the sodium salt of 1,8-octanedisulfonate,[32] and [CpFe(1,4-dicholorobenzene)][$PF_6$][33] were prepared according to published procedures. All solvents and other starting materials were purchased as ACS grade from Aldrich and were used as received. Metal salts of the sulfonic acids were converted to the acid form by passing them through an Amberlyst 36(wet) ion-exchange column. **$G_2$NDS**, **$G_2$BPDS**, **$G_2$ADS**, and **$G_2$ODS** precipitate, as acetone clathrates, by direct reaction of guanidinium tetrafluoroborate, prepared by neutralization of guanidinium carbonate with tetrafluoroboric acid, with the corresponding disulfonic acid in acetone. These compounds readily lose enclathrated acetone under ambient conditions to yield pure guanidinium organodisulfonate apohosts. The compounds reported here were crystallized from methanolic solutions containing the dissolved apohost and the corresponding guest where applicable. The stoichiometries of the resulting inclusion compounds tend to be independent of the host:guest stoichiometric ratios during crystallization. The stoichiometries of all inclusion compounds were confirmed by $^1$H NMR spectroscopy in addition to single-crystal structure determinations. $^1$H NMR spectra were recorded on a Varian INOVA 200 MHz spectrometer.

**[Guanidinium]$_2$[1,4-benzenedisulfonate], $G_2$BDS.** [CpFe(1,4-dicholorobenzene)][$PF_6$] (2.50 g, 6.05 mmol) was added to a 200 mL aqueous solution containing 7.65 g (60.7 mmol) of $Na_2SO_3$. The mixture was refluxed, in the absence of light, for several hours at which point the iron compound had completely dissolved. The resulting solution was photolyzed, with several intermittent filtrations, in direct sunlight for several days. The resulting nearly clear solution was treated with $BaCl_2$(aq), and the $BaSO_3$ precipitate removed by centrifugation, until a precipitate no longer formed. Any excess barium can be precipitated as $BaSO_4$ by the addition of small amounts of $H_2SO_4$. After centrifugation, the cloudy solution was filtered through Celite and evaporated to give a crude mixture of mostly sodium 1,4-benzenedisulfonate and NaCl. The solid was redissolved in water and passed through an Amberlyst 36(wet) ion-exchange column, after which the water was evaporated and the residue dissolved in acetone. Treatment of this solution with an acetone solution of **G**[$BF_4$] resulted in the immediate precipitation of **$G_2$BDS·**(*acetone*), which was filtered and dried under vacuum to give 1.41 g (3.96 mmol) of pure, white **$G_2$BDS** apohost (65% yield). $^1$H NMR (dimethyl sulfoxide-$d_6$, 200 MHz, *J*/Hz): $\delta$ 7.42 (s, 4H, Ar-*H*), 6.93 (s, 12H, **G**).

**[Guanidinium]$_2$[mesitylenedisulfonate], $G_2$MDS.** Chlorosulfonic acid (6.36 mL; 11.1 g, 95.7 mmol) was added slowly via syringe to a chilled (−15 °C) round-bottom flask containing 50 mL of anhydrous chloroform and 5.00 g (5.79 mL; 41.6 mmol) of mesitylene, all under a nitrogen atmosphere. After 15 min, the chloroform and excess chlorosulfonic acid were decanted from the oily residue. The oil was further rinsed with chloroform (20 mL), dissolved in acetone, and then treated with an acetone solution of **G**[$BF_4$]. The **$G_2$MDS·**(*acetone*)$_n$ precipitate was filtered and dried under vacuum to give 3.47 g (8.73 mmol) of pure **$G_2$MDS** (21% yield). $^1$H NMR (dimethyl sulfoxide-$d_6$, 200 MHz, *J*/Hz): $\delta$ 6.96 (s, 12H, **G**), 6.68 (s, 1H, Ar-*H*), 2.80 (s, 3H, 2-C$H_3$), 2.44 (s, 6H, 4,6-C$H_3$).

**[Guanidinium]$_2$[2-methoxy-4,6-dimethyl-1,5-benzenedisulfonate], $G_2$MDBDS.** Chlorosulfonic acid (5.62 mL; 9.83 g, 84.4 mmol) was added slowly via syringe to a chilled (−15 °C) round-bottom flask containing 100 mL of anhydrous chloroform and 5.00 g (5.19 mL; 36.7 mmol) of 3,5-dimethylanisole, all under a nitrogen atmosphere. After thirty minutes, the chloroform was evaporated and the oily residue dissolved in acetone. The solution was then treated with an acetone solution of **G**[$BF_4$] to precipitate **$G_2$MDBDS·**(*acetone*)$_n$ as a white powder. The precipitate was filtered and dried under vacuum to give 4.27 g (10.3 mmol) of pure **$G_2$MDBDS** apohost (28% yield). $^1$H NMR (dimethyl sulfoxide-$d_6$, 200 MHz, *J*/Hz): $\delta$ 6.97 (s, 12H, **G**), 6.53 (s, 1H, 3-*H*), 3.64 (s, 3H, OC$H_3$), 2.76 (s, 3H, 6-C$H_3$) 2.47 (s, 3H, 4-C$H_3$).

**[Guanidinium]$_2$[4,4′-phenyl Etherdisulfonate], $G_2$PEDS.** Chlorosulfonic acid (4.43 mL; 7.88 g, 67.6 mmol) was added slowly via syringe to a chilled (−15 °C) round-bottom flask containing 20 mL of anhydrous chloroform and 5.00 g (4.66 mL; 29.4 mmol) of phenyl ether, all under a nitrogen atmosphere. After fifteen minutes, the chloroform and excess chlorosulfonic acid are decanted from the oily residue. The oil was further rinsed with chloroform (20 mL), dissolved in acetone, and then treated with an acetone solution of **G**[$BF_4$]. The **$G_2$PEDS·**(*acetone*)$_n$ precipitate was filtered and dried under vacuum to give 9.22 g (20.5 mmol) of pure, white **$G_2$PEDS** (70% yield). $^1$H NMR (dimethyl sulfoxide-$d_6$, 200 MHz, *J*/Hz): $\delta$ 7.62 (d, 4H, $^2J$ = 12, 2-*H*), 6.96 (d, 4H, $^2J$ = 12, 3-*H*), 6.92 (s, 12H, **G**).

**Crystallography.** Experimental parameters pertaining to the single-crystal X-ray analyses are given in Table 1 (see Supporting Information). Data were collected on either Siemens or Bruker CCD platform diffractometers with graphite monochromated Mo K$\alpha$ radiation ($\lambda$ = 0.71073 Å) at 173(2) K. The structures were solved by direct methods and refined with full-matrix least-squares/difference Fourier analysis using the SHLEX-97 suite of software.[34] All non-hydrogen atoms were refined with anisotropic displacement parameters and all hydrogen atoms were placed in idealized positions and refined with a riding model. Data were corrected for the effects of absorption using SADABS.

**Acknowledgment.** This work was supported in part by the MRSEC program of the National Science Foundation under Award Number DMR-9809364 and the NSF Division of Materials Research (DMR-9908627). K.T.H. also gratefully acknowledges a postdoctoral fellowship from NSERC of Canada.

**Supporting Information Available:** X-ray experimental details in the form of a crystallographic information file (CIF) have been deposited. This material is available free of charge via the Internet at http://pubs.acs.org.

JA0030257

(31) Acquavella, M. F.; Evans, M. E.; Farraher, S. W.; Névoret, C. J.; Abelt, C. J. *J. Org. Chem.* **1994**, *59*, 2894−2897.

(32) Stone, G. C. H. *J. Am. Chem. Soc.* **1936**, *58*, 488.

(33) Khand, I. U.; Pauson, P. L.; Watts, W. F. *J. Chem. Soc.* (*C*) **1968**, 2261.

(34) *SHELX*-97, G. M. Sheldrick, University of Göttingen, 1997.